Mater.Phys.Mech.2 (2000) 1-9

MICROSTRUCTURAL ASPECTS OF HIGH AND LOW T_C SUPERCONDUCTORS

Chandra S. Pande

Materials Science and Technology Division, Naval Research Laboratory, Washington, DC 20375-5343

Received: July 7, 2000

Abstract. The U.S. Navy has been developing superconducting homopolar motors for ship propulsion since 1969, initially using conventional NbTi superconducting material for the magnets. With the advent of high critical temperature (high T_c) superconductors, NbTi has been replaced by bismuth-strontium-calcium-copper-oxide (BSCCO). Performance of these motors depends critically on the properties of the superconducting material specifically of the magnitude of the current density and its stability with time. Flux creep is a major concern in these materials, since it limits high T_c superconductor performance at temperatures above about 30K. As is well known these properties are strongly influenced by the high T_c superconductor microstructure. The level of current transport in a given high T_c superconductor depends upon several intrinsic microstructure-property relationships. In the typical orthorhombic crystal structure, superconducting current flows primarily in the *a-b* planes. In polycrystalline materials, superconducting current drops off as grain boundary misorientation increases. High current densities in polycrystalline materials needs strong *c*-axis alignment where current is expected to flow through those grains connected by low angle boundaries. When a magnetic field is applied, the flux vortices may shift due to the force from the current or to thermal activation, resulting in a loss of superconducting properties known as flux creep. Flux vortices may be pinned by microstructural defects such as grain boundaries or dislocations, if present in sufficient quantities, hence the importance of microstructure. The present paper deals with the microstructural aspects of superconductivity, specifically the role played by microstructure in determining superconducting properties. Examples from both the low and high T_c materials will be cited and future trends discussed.

1. INTRODUCTION

Superconducting materials are finding increasing use in the generation of high magnetic fields, in lossless electrical power transmission and storage, in magnetic sensors, in electromagnetic radiation detectors and in high speed digital signal and data processing. Since the discovery of superconducting materials with a T_c above the boiling point of liquid nitrogen (78K) these materials are roughly divided into two categories, *viz.,* low and high T_c superconductors. In this paper microstructure and their relationship to superconducting properties are briefly considered. For a more detailed coverage references are cited as appropriate.

Superconductivity was discovered by H. Kamerlingh Onnes [1]. He also discovered that superconductivity was destroyed by the application of a sufficiently strong magnetic field or on the passage of sufficiently strong electrical current. The transition from superconducting to normal state can be sharp (Type I superconductors) or broad (Type II superconductors). The strength of the magnetic field needed to bring out the transition is called the thermodynamic critical field H_c. With the exception of vanadium and niobium all the superconducting elements and most of their alloys are type I superconductors. Most of the practical materials are type II. In these materials microstructure plays an important role. The theory of type II superconductivity was given by Ginsburg, Landau, Abrikosov and Gorkov and is usually called GLAG theory. These researchers showed that the type I or type II behavior is determined by the ratio $\kappa = \lambda_L / \xi$ where λ_L is the London penetration depth and ξ is the coherence length. Typically, this ratio, κ, is less than $(2)^{1/2}$ for type I and greater than $(2)^{1/2}$ for type II superconductors. For more details see for example reference [2].

Corresponding author: C.S. Pande, e-mail: pande@anvil.nrl.navy.mil

In type II superconductors the magnetic field penetrates the material slowly at a value denoted by H_{c1} and continues up to a value denoted by H_{c2} at which point the material is transformed to normal (non-superconducting) state. The superconducting state between H_{c1} and H_{c2} is called mixed state. Type II behavior is shown in general by many alloys and compound superconductors. Abrikosov showed mixed state forms flux tubes (called flux lines, fluxiods or vortices). It turns out that these tubes form a triangular lattice that can be observed. The flux tubes are parallel to the magnetic field. As the field is increased the fluxiods get closer and closer till at H_{c2} the cores of the fluxiods which are normal completely overlap and the whole specimen becomes normal i.e. non-superconductive.

Whenever a current J flows in a superconductor in mixed state, it experiences a Lorentz force, F_L. This acts in a direction perpendicular to both B (which is parallel to flux line) and J. This force can move the fluxiods, and create an electric field E and produce a resistance in the superconductor (=E/J), unless the fluxiods are prevented from moving *i.e.,* are pinned by some microstructural feature. The critical current J_c is that current that produces enough F_L to depin the fluxiods and make them move. It is thus clear that to optimize J_c one needs microstructure that can pin fluxiods strongly. Since high J_c is a prime requirement for most of the technological applications, the prime importance of suitable microstructure is obvious.

To obtain an expression of the pinning force (and hence J_c), in terms of microstructure one needs to obtain the local or “elementary” pinning force between the fluxiod and the pinning center and then sum over the entire flux line lattice. Summation over such elementary pinning forces is still a matter of controversy. It is especially difficult if several mechanisms are operating, or if the system contains several classes of pinning agents. See references [3] and [4] for more details.

Radiation is also a convenient way to introduce a desired microstructure and then study their correlation with basic properties of superconductors. Radiation produces three major effects in a superconductor. There may be a change in critical current, and a change in transition temperature and thirdly there is usually an increase in normal state electrical resistivity. The nature of defects produced are (1) point defects, produced by almost all radiations, (2) cascades usually produced by high energy neutrons, protons and ions, (3) dislocation loops and voids, both of which usually are results of annealing, and (4) anti-site or disorder defects *i.e.* atoms occupying wrong positions without change of overall structure. Obviously this applies to ordered structures only. For further information see reference [5].

In next sections, we describe some of the most important superconducting materials, their microstructure and their properties.

2. NIOBIUM-TITANIUM ALLOY SUPERCONDUCTORS

A majority of superconducting magnets are constructed out of Nb-46-50 wt.% Ti alloy (Nb-47 wt.% Ti being most common) and the process is now commercially well established. The reason for this preference is the ease of fabrication and excellent mechanical properties. NbZr alloys have comparable critical current to NbTi which could be very high (for NbTi typically J_c~$3\cdot10^9$ Ampere/meter^2 at 5 Tesla and at 4.2K). Such a high J_c is achieved by developing processing procedures to produce strong pinning centers. As with some other practical superconductor, commercial NbTi superconductors is almost always produced in multifilamentary form, with up to 5000 filaments in a wire typically 0.5 to 2 mm in diameter.

The main flux pinning centers [6,7] in this material are α-titanium precipitates with hexagonal close packed structure and to a lesser extent dislocation cells introduced by plastic deformation. The α-titanium precipitation is usually carried out at 375 – 420 °C. The *w*-phase precipitation can also occur during this heat treatment but is usually avoided by suitable cold work. Although *w*-phase provides strong pinning it reduces wire drawability [8]. The single heat treatment mentioned above will produce a maximum amount of precipitate of about 10% (by volume). This is often not sufficient to produce the critical current the material is capable of. A series of strains given to the material followed by heat treatment can increase this volume fraction to up to 20%. Care has to be taken not to increase the size of the α-precipitates beyond their typical size which ranges between 80 nm to 200 nm, or to reduce the titanium content of the matrix below about 36 wt.%. It should be noted that although initially the α-precipitates are randomly distributed and roughly spherical in shape the precipitates are elongated, the drawing axes due to subsequent deformations, till by the final treatment, in modern practical wires they are highly distorted into densely folded sheets, and until they are only about 1 nm thick, separated by only a few nm, and made up of long strands [9,10].

Because of two competing mechanism of pinning due to precipitates and interfaces (grain bound-

aries and cell boundaries) it is difficult to separate the contribution of each mechanism. However it is now accepted that the pinning is nearly proportional to the volume fraction of precipitates, and is inversely proportional to the cell size or grain size. The proportion of the pinning centers depend on the processing conditions. It is found that at the optimum wire size, the density of the precipitates is about ten times the density of grain boundaries [11].

Fabrication of NbTi conductors for practical applications are usually in the form of multifilametary filaments [4].

3. A15 SUPERCONDUCTORS

A15 superconductors are those with A15 type structure (sometimes also known as Cr_3Si structure or "β tungsten" structure) [4], the most well known being Nb_3Sn, V_3Si [12] and V_3Ga compound superconductors. Another A15 superconductor, Nb_3Ge, had the record for highest transition temperature [13] before the advent of high T_c superconductors. About 76 A15 compounds are known to exist. The typical compound A_3B is close to the stoichiometric ratio of 3:1. The A atoms (A = Nb, V, Mo, Ti, etc.) are on the faces of a cube, formed by B atoms (Ga, Sn, Si, Au, Pt, etc.) which occupy the bcc positions of the cube. The A atoms form three orthogonal chains in the crystal parallel to three <100> directions as shown in Fig. 1. The nearest neighbor distance along the chain is less than the distance of closest approach in a pure A crystal. For example in Nb_3Ge the distance between the Nb atoms along the chain is 0.2575 nm compared to 0.2858 nm in Nb bcc unit cell [4].

The microstructure observed in A15 materials are grain boundaries, precipitates, radiation induced defects and a low density of dislocations [14]. Of these grain boundaries are the most important. Grain boundaries are responsible to a great extent for the high value of critical current J_c observed in these materials. This relationship between J_c and grain size D has been studied by many workers. [15,16,17,18]. Grain size can be altered by varying the growth conditions. It is then found that J_c increases linearly with the inverse of grain size sometimes reaching a maximum. Grain size can in fact be made as small as 30 nm in A15 materials by suitable annealing.

So far there is no good model that provides a detailed mechanism by which grain boundaries pin flux line lattice. Since Kramer's model [19] is extensively used in analyzing J_c observations we provide a brief outline of this model. The basic premise

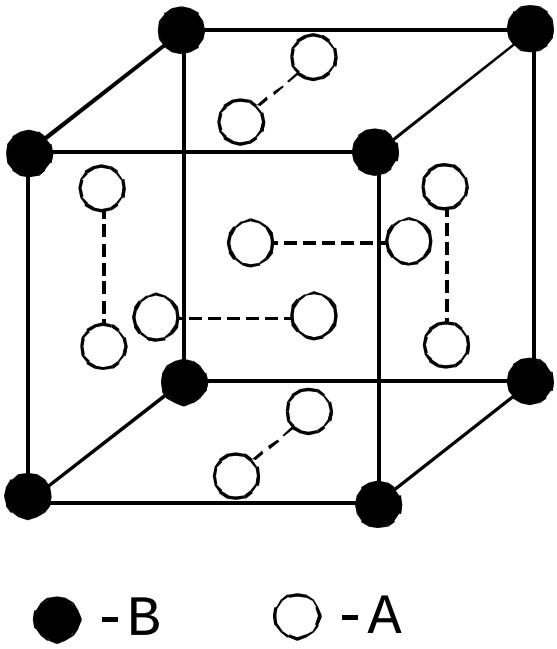

Fig.1. A15 structure.

in Kramer's model is that the depinning force is such that it exceeds the shear strength of the flux line lattice. Then the flux flow will occur by shear. Kramer then utilized the idea of the shearing of a real lattice. On such considerations he obtains a relation for flux pinning as

$$J_c H = \frac{13 \cdot 10^{10} H_{c2}^{5/2} b^{1/2} (1-b)^2}{\kappa^2 \left(1 - \frac{a_0}{D}\right)^2}, \qquad (1)$$

where a_0 is the flux line lattice constant, D is grain size, $b = H/H_{c2}$ (reduced magnetic field) and with k as defined before. Kramer's model has been criticized by Dew-Hughes [20]. It certainly does not predict correct grain size dependence.

We now briefly mention the model of Pande and Suenaga [21] where grain size dependence is considered in detail. This model is based upon the following assumptions: (1) any grain boundary segment is regarded to be made up of a superposition of uniformly spaced dislocation walls spacing and other parameters are so chosen to satisfy all boundary conditions where on the average, the Burgers' vector are randomly distributed along all three axes; (2) grains are made up of such segments, the relation between the grain size D, and grain segment, d, will depend on geometry and shape of the grain, but on the average $D \approx kd$ where k is of the order of 2; and (3) the flux pinning is primarily due to first order elastic interactions. Based on the above assump-

tions and after statistically summing the elementary pinning forces an expression for grain boundary pinning was obtained as

$$F_p(D) = \frac{P_0(1-b)^2}{a_0}\frac{a_0}{D}\sin^2\left(\frac{\pi}{\sqrt{3}k}\frac{D}{a_0}\right), \qquad (2)$$

where $k \approx 2$, P_0 is a constant independent of grain size D, b is the "reduced" magnetic field and a_0 is the lattice constant of the flux line lattice which depends on the magnetic field. Eq. 2 shows that the flux pinning and hence critical current is approximately inversely proportional to grain size as expected from experiments. However, Eq. 2 also gives an oscillatory behavior in F_p as function of grain size. Such oscillations are not observed experimentally although experimental results do show large scatter in the data, especially in thin films. We believe that such an oscillatory behavior can be removed if a distribution in grain sizes is taken into account. Pande [22] by his measurements of grain sizes in Nb_3Sn found that the distribution is roughly lognormal. It is seen that the oscillations are smoothed out but there is a peak in the F_p at a value of $a_0 / D = 1.83/k$. The exact location of the peak will depend on the value k used. This leads to the conclusion that flux pinning cannot be indefinitely increased by grain refining.

An interesting feature of A15 superconductors is the relation between its properties (especially T_c) with long-range crystallographic order, S. A convenient measure of S is the Bragg-Williams order parameter S. This parameter is such that for complete order S=1 and for complete disorder S=0. It is known that in A15 with T_c is usually highest for S=1 and gradually decreases as $S \approx 0$. This is dramatically seen when the order parameter is gradually reduced on irradiation. The effect of composition changes upon T_c can also be described in a similar fashion, by now one needs two order parameters S_A and S_B for A and B lattice sites respectively. When B is a transition element the sensitivity to long range order is much less [4].

Apart from anti-site defects (A atom on B site and B atom on A site) it has been shown that depending on the nature of radiation, other defects are also created. High-energy neutron or ions have been shown to create highly disordered regions [23] of the size 2 to 6 nm depending on the energy. Some dislocation loops are also observed. Disordered regions of the same order in size as coherent length may play significant role in determining both J_c and T_c of the irradiated A15 superconductors. Most of the A15 materials are brittle and fail by cracking along grain boundaries. Hence it is difficult to produce dislocations by mechanical deformation at low temperatures. Some ingrown dislocations have been observed in Nb_3Sn and V_3Si. The Burgers vector [24] of these dislocations are of the type b = [100]. However dislocations play only a minor role in determining either superconducting or normal properties of A15 materials.

Other low T_c superconductors are nitride and carbonitride superconductors with cubic $B1$ (sodium chloride) structure [25] and organic superconductors [26,27] (most if not all of these molecules contain sulfur or selenium atoms additions to the parent molecule tetrathiafulralene (TTF)) doped C_{60} fullerene superconductor [28,29] and Chevrel phase superconductors [30,31].

The main microstructural features responsible for high critical currents in these materials appear to be grain boundaries and point defects.

4. HIGH T_c SUPERCONDUCTORS

High T_c superconductors are oxide superconductors, with perovskite structure. Before their discovery superconductivity was unknown in copper oxides. In 1986 Bednorz and Muller [32] observed evidence of superconductivity with transition temperature over 30K in $La_{2-x}Ba_xCuO_4$. This material had perovskite structure. A substitution of yttrium for lanthanum led to the discovery of $YBa_2Cu_3O_{6+\delta}$ (δ<1) often referred to as YBCO or 123 because of the ratio of Y:Ba:Cu in this material. This was the first superconductor discovered with a T_c in the range 90-95K, [33] well above the boiling point of liquid nitrogen. This discovery was followed in 1988 by the discovery of bismuth ($Bi_2Sr_2Ca_2Cu_3O_{10+\delta}$) and thallium ($Tl_2Ba_2Ca_2Cu_3O_{10+\delta}$) based superconductors with even higher T_c. A large family of these superconductors with over 40 members are now known.

BSCCO family of superconductors have also perovskite type structure with copper oxide planes and chains and orthogonal unit cells. Two most common members are $Bi_2CaSr_2Cu_2O_{8+\delta}$ (δ<1) commonly known as 2122 or 85K phase, and $Bi_2CaSr_2Cu_3O_{10+\delta}$ commonly known as 2223 or 110K phase. Thallium superconductors have similar structure. The highest T_c in this family is 125K. With the increasing number of CuO planes the T_c seems to increase in the oxide superconductor family. For details about the structure see reference [34].

After the discovery of high T_c superconductors, they have been subjected to intense investigations to determine microstructure present in them using transmission electron microscopy and related tech-

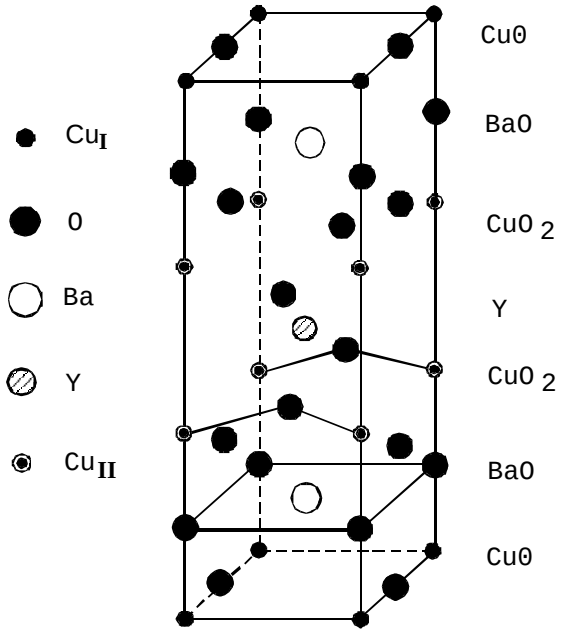

Fig.2. High T_c perovskite structure $YBa_2Cu_3O_7$.

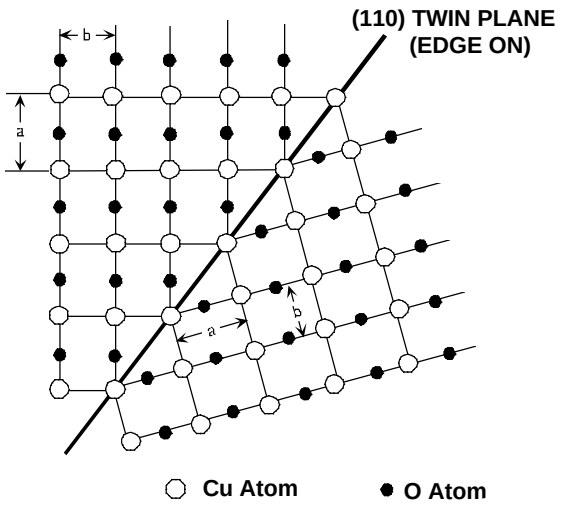

Fig.3. Twin structure in high T_c materials.

niques. Relation between structure, microstructure and normal and superconducting properties have also been determined in many cases. Of course, as in conventional superconductors the microstructure present in oxide superconductors is expected to play a prominent role in determining the current carrying capacity of these materials. It is now known that the important defects in these superconductors include twin and grain boundaries, point defects and impurities, dislocations and stacking faults precipitates (second phase particles) voids and microcracks.

Planar defects [35,36] were discovered in $YBa_2Cu_3O_{7-\delta}$ (δ<0.5) almost immediately after the discovery of this superconductor using transmission electron microscopy. They were shown to be twin boundaries. The planar defects are (110) twin interfaces. The twin formation is due to a tetragonal to orthorhombic phase transformation that this material undergoes below about 750 °C. If *a* and *b* denote the lattice parameter (which are equal when the crystal is in tetragonal form), Pande *et al.* [36] have shown that twin misorientation θ is given by

$$\theta = 4\tan^{-1}\left[\frac{a-b}{a+b}\right], \tag{3}$$

$$\approx 4\frac{a-b}{a+b} \quad since \quad a \approx b. \tag{4}$$

Using the appropriate values of *a* and *b*, it is found that θ is about one degree in good agreement with the splitting observed in electron diffraction. Because of this twinning relation the twins give the alternate black and white contrast observed in TEM. Sometimes a fine tweed-like structure is also observed instead. This structure has been shown to consist of fine (<5 nm) orthorhombic domains each with a twin like crystallographic relation with its neighbor. The twins can sometimes form in two sets of colonies parallel to either (110) or ($1\bar{1}0$) direction. The twin spacing varies somewhat is usually is of the order of 100 nm.

The twin formation can be understood as due to a need to accommodate shape change resulting from the tetragonal to orthorhombic transformation as shown in Fig. 3. The need to accommodate *i.e.*, to reduce strain energy however must be balanced by the need to use as few twinning surfaces as possible. The twin spacing *d* can thus be obtained by minimizing the sum of strain energy (proportional to *d*) and surface energy (which is proportional to 1/*d*).

Twin boundaries are planar defects and are found in sufficient densities in many specimens and are therefore expected to influence J_c in these materials. There is some evidence that this is indeed so [37]. J_c in twinned single crystals was found to be higher than in the same crystal made twin free by the application of appropriate pressures. Also evidence of pinning by twin boundaries have been found by decoration techniques [38]. Theoretical calculation predicting a relation between twin interfaces and flux pinning is now available, but need experimental verification.

Most high T_c materials show microcracks which are probably produced during processing. In the case

of YBaCuO, the tetragonal to orthorhombic transformation produces stresses that are reduced in *a-b* plane by twin formation. However there can be some shrinkage along *c*-axis, which can be relieved by microcracks. Microcracks can pin fluxiods, but they are not in sufficient number to contribute significantly to J_c. It is known that dispersion of Ag in these materials reduces cracking, but J_c is hardly affected, supporting the above conclusions.

Dislocation densities observed in high T_c materials like $YBa_2Cu_3O_7$ is usually low ($<10^5$ cm/cm^3). Unless introduced by deformation the commonly observed (by TEM) dislocations are perfect dislocations with a [100], [010], or [110] Burgers vector. The slip plane is always found to be (001) i.e. the *a-b* plane. The dislocations density can be increased somewhat by deformation processes, especially at elevated temperatures, but their role in determining both normal and superconducting properties is rather limited.

All Bi based superconductors exhibit superstructure modulation, which is not commensurate with the basic structure. [39]. These modulations are also expected to alter the J_c in these materials but the flux pinning mechanism has not as yet been worked out.

4.1 Critical Current in High T_c Polycrystals

It is well established that the critical current of even carefully prepared polycrystalline high T_c material is extremely low (in the range of 100-1000 Å/cm^2 at 77K). This value drops further in the presence of even a small magnetic field of a small fraction of a Tesla. On the other hand the J_c value for single crystals, in bulk as well as in thin film form, is at least three orders of magnitude higher.

This limitation in critical current is due to the behavior of the grain boundaries as a “weak link” or *i.e.*, having a Josephson coupling between the grains [40]. Much higher value of critical current J_c of single crystals in bulk as well as in thin films $YBa_2Cu_3O_7$ compared with polycrystals of the same material suggests strongly the degrading role of grain boundaries. Two papers by Dimos and co-workers [41,42] have firmly established that J_c is a very sensitive function of the grain boundary at least in thin films. However recent experimental results indicate this may not be true for all boundaries [43]. Due to the presence of grain boundaries in polycrystals, which act as weak links, sintering alone cannot give high J_c values. Also weak link behavior is largely intrinsic, a better way to enhance J_c is by texturing. Salama *et al.* [44] had reviewed in 1992 different processes which has been tried to produce practical superconductors with high J_c. In all cases the aim has been to produce materials that has highly textured. Additional challenge is to produce long length of these materials with mono or multifilaments. Some of the techniques that has been at least partially successful. These are, dip coat technique [45], multilayer tape by continuous heat treatment, melt texturing and powder in tube method [46,47]. Many of these methods have also benefited by the use of silver, as the metal in the metal / superconductor composite. Many other factors control the critical current in these materials. These are oxygen content, porosity, grain growth, lattice defects and volume and size distribution of second phase. However it is the grain alignment or specifically the *c*-axis texture and *a-b* grain alignment that seems to be most critical. A biaxial alignment of adjacent grains appears to be a necessity with the majority of grains joined by low angle boundaries. In case of BSCCO systems on the other hand it has been claimed that a macroscopic *c*-axis alignment is enough to give high critical currents. The two requirements can however be reconciled in principle. For example in the practical superconductors of BSCCO system showing high J_c it has been reported that they are composed of colonies of grains aligned along the *c*-axis but *c*-axis twist misaligned. X-ray texture studies which provide a convenient orientation maps are very useful for ascertaining these microstructure.

We have conducted a detailed study of the texture in BSCCO material whose superconducting properties have been also characterized. In particular both the critical currents and the decay of magnetization were measured. The aim being to determine the nature of the grain morphology and its relationship with current carrying capacity. The Bi2212 grain texture was evaluated from pole figure data, with (001) pole figures from (008) reflections used for *c*-axis texture and (115) pole figures used for *a-b* axis texture [47]. For each pole figure, X-ray intensities were measured at the appropriate 2° angle for the reflection as the specimen was tilted and rotated in a spiral pattern. The tilt angle was varied continuously between 0 and 80° at 2.5° per revolution. The rotation angle was incremented simultaneously; X-ray intensities were summed over 6° of rotation in a time period of 8 seconds. From these data, the texture software produced pole figures in the form of X-ray intensity contour plots. Current transport properties and values for *c*-axis texture of the silver-Bi2212 tapes have been reported previously [47].

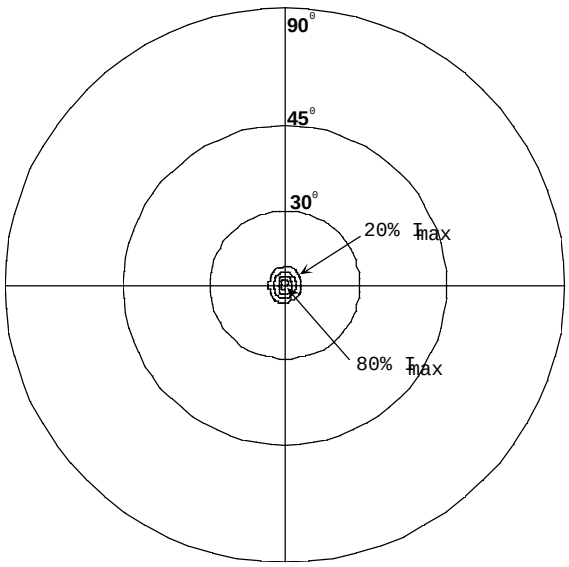

Fig. 4. Contour plot at half of the maximum peak intensity from the (001) pole figure illustrating the distribution of the pole population.

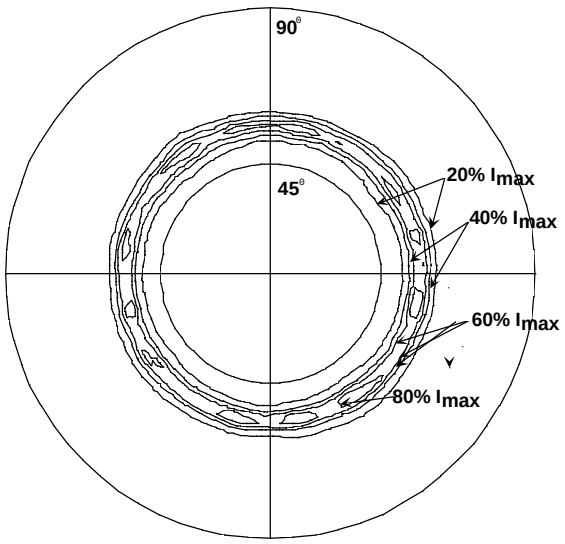

Fig. 5. (115) ϕ scans at 2.5 and 58° tilts from a circular specimen of a surface coated silver-Bi2212 tape,showing the pole orientation distribution.

The tapes given melt processing treatments had overall critical current densities more than an order of magnitude higher than that of the tape given the lower temperature treatment. Representative values for *c*-axis texture were determined from (001) pole figures developed from (008) reflections. The (001) pole figure for sample of the surface coated silver-Bi2212 tapes is given in Fig. 4 as a contour plot with contour levels at the stated percentages of the maximum peak height. Since the X-ray intensity is strongly clustered in the center of the figure, most of the Bi2212 grains were oriented so that their c axes were nearly perpendicular to the surface of the tape. This strong *c*-axis texture was exhibited by all of the tapes given melt processing treatments. The *c*-axis angular distributions for the tapes given melt processing treatments are one third of the value for the tape given the lower temperature treatment. It should be noted that the *c*-axis texture determined from these (001) pole figures is global rather than local in nature, since the data from which the pole figures were developed were obtained from most of each tape surface.

The *a-b* axis texture of the Bi2212 grains was evaluated from (115) pole figures. The (115) pole figure for a sample of the surface coated silver-Bi2212 tapes is shown in Fig. 5. The regions of the ring with higher X-ray intensity are not arranged with four-fold symmetry. The *a-b* axis orientation for the Bi2212 grains in the sample is random on the basis of the overall Bi2212 layer. The other silver-Bi2212 tapes displayed the same type of random *a-b* axis orientation in a global sense. These results are consistent with the findings of Goyal *et al.* [48] for silver sheathed Bi2223 tapes with strong *c*-axis texture, a high fraction of low angle grain boundaries was observed in spite of no detectable *a-b* axis texture [48]. This type of local, preferred *a-b* axis orientation should improve critical current densities in BSCCO tapes with strong *c*-axis texture, whether current flow is percolative in nature [49] or occurs according to the freeway model [50].

This was one of the few studies where both the *c*-axis texture and *a-b* texture has been measured on the same specimens and their superconducting properties have also been correlated [47]. There is a good correlation between the c-axis texture and J_c. Surprisingly on a global basis the system showed little *a-b* texture. However the material did give indications of local *a-b* texture in addition to *c*-axis texture. These results are consistent with the model of grain morphology as proposed by Riley and coworkers [49]. The microstructure of these materials as for as the grain morphology is concerned can be explained in terms of colonies of grains. Inside a typical colony the grains differ mostly in their small amount of twist along *c*-axis, the *c*-axis being almost common. The precise prediction of superconducting current flow though such a complicated microstructure remains a major challenge but preliminary results have provided some guidelines. The maximum current reported in the type of tapes investigated in the present study is still at least a factor of ten less than that of single crystals. The

spread of *c*-axis tilt spread as well as the spread of *c*-axis twist contributes to this degradation but the major bottleneck for the flow of the current is in the structure of grains or grain boundaries that connect these colonies. Our results can not be easily extrapolated to YBCO system which may differ in their grain morphology from BSCCO.

Finally we should mention that high T_c materials show current instability thousands of time worse than low T_c materials, due to the instability of the vortex lattice in these materials on the introduction of magnetic field. The phenomenon is called flux creep. It prevents the use of these materials at sufficiently high temperature and magnetic fields. Flux creep is closely tied to the underlying microstructure of the material. Pande and Masumura [51] have derived exact expression for magnetic relations in high T_c superconductors for thermally activated flux motion model assuming a distribution of activation energies. The results are compared with experiments and shown to be in excellent agreement with experiments. Determining these activation energies from the microstructure remains a formidable challenge.

REFERENCES

[1] H. Kamerlingh Onnes // *Proceedings from the Section of Sciences (Amsterdam)* **14** (1911) 113-115 and 818-821.

[2] M. Tinkham, *Introduction to Superconductivity* (McGraw Hill, New York, 1975).

[3] A. M. Campbell and J. E. Evetts // *Adv. Phys.* **21** (1972) 199.

[4] *Metallurgy of Superconducting Materials*, ed. by T. Luhman and D. Dew-Hughes (Academic Press, New York, 1979).

[5] *Physics of Irradiation Effects in Crystals*, ed. by R. A. Johnson and A. N. Orlov (North Holland, Amsterdam, 1985).

[6] I. Pfeiffer and H. Hillmann // *Acta Metall.* **16** (1968) 1429.

[7] D. C. Larbalestier and A. W. West // *Acta Metall*. **32** (1984) 1871.

[8] M. I. Buckett and D. C. Larbalestier // *IEEE Trans. Mag*. **23** (1987) 1638.

[9] P. J. Lee and D. C. Larbalestier // *Acta Metall*. **35** (1987) 2526.

[10] P. J. Lee, J. C. McKinnell and D. C. Larbalestier // *IEEE Trans*. Mag. **25** (1989) 1918.

[11] C. Meingast and D. C. Larbalestier // *J. App. Phys.* **66** (1989) 5971.

[12] G. F. Hardy and J. D. Hulm // *Phys. Rev.* **89** (1953) 884.

[13] J. R. Gavaler // *App. Phys. Lett*. **23** (1973) 480.

[14] C. S. Pande, In: *Metallurgy of Superconducting Materials* ed. by T. Luhman and D. Dew Hughes (Academic Press, New York, 1979).

[15] E. Nembach and K. Tachikawa // *J. Less Common Met.* **19** (1969) 359.

[16] R. M. Scanlan, W. A. Fietz and E. F. Koch // *J. App. Phys.* **46** (1975) 2244.

[17] B. J. Shaw // *J. App. Phys.* **47** (1976) 2143.

[18] A. W. West and R. D. Rawlings // *J. Mater. Science* **12** (1977) 1962.

[19] E. J. Kramer // *J. App. Phys*. **44** (1973) 1360.

[20] D. Dew Hughes // *Phil. Mag*. **55** (1987) 459.

[21] C. S. Pande and M. Suenaga // *App. Phys. Lett.* **29** (1976) 443.

[22] C. S. Pande, unpublished work.

[23] C. S. Pande // *Solid State Commun.* **24** (1977) 241.

[24] S. Mahajan, S. Nakahara, J. H. Wernick and G. Y. Chin, unpublished work.

[25] L. E. Toth, *Transition Metal Carbides and Nitrides* (Academic Press, New York, 1971).

[26] J. M. Williams, A. J. Schultz, U. Geiser, K. D. Carlson, A. M. Kini, H. H. Wang, W. K. Kwok, M. H. Whangbo and J. E. Schirber // *Science* **252** (1991) 1501.

[27] A. E. Underhill // *J. Mater. Chem.* **2** (1992) 1.

[28] H. W. Kroto, J. R. Heath, S. C. O'Brien, R. F. Curl and R. E. Smalley // *Nature* **318** (1985) 162.

[29] A. F. Hebard, M. J. Rosseinsky, R. C. Haddon, D. W. Murphy, S. H. Glarum, T. T. M. Palstra, A. P. Ramirez and A. R. Kortan // *Nature* **350** (1991) 600.

[30] R. Chevrel, M. Sergent and J. Prigent // *J. Solid State Chem*. **3** (1971) 515.

[31] B. T. Matthias, M. Marezio, H. E. Barz Corenzwit and A. S. Cooper // *Science* **175** (1972) 1465.

[32] J. G. Bednorz and K. A. Muller // *Z. Phys. B* **64** (1986) 189.

[33] M. K. Wu, J. R. Ashburn, C. J. Torng, P. H. Hor, R. L. Meng, L. Gao, Z. J. Huang, Y. Q. Wang, C. W. Chu // *Phys. Rev. Lett* **58** (1987) 908.

[34] *Chemistry of Superconducting Materials*, ed. by T. A. Vanderah (Noyes Publications, Park Ridge, NJ, 1992).

[35] R. Beyers, G. Lim, E. M. Engler, R. J. Savoy, T. M. Shaw, T. R. Dinger, W. J. Gallaghar and

R. L. Sandstrom // *App. Phys. Lett.* **50** (1987) 1918.
[36] C. S. Pande, A. K. Singh, L. E. Toth, D. U. Gubser and S. A. Wolf // *Phys. Rev. B* **36** (1987) 5669.
[37] C. H. Chen, J. Kwo and M. Hong // *App. Phys. Lett.* **52** (1988) 841.
[38] P. L. Gammel, D. J. Bishop, G. J. Dolan, J. R. Kwo, C. A. Murray, L. F. Schneemeyer and J. V. Waszczak // *Phys. Rev. Lett.* **59** (1987) 2592.
[39] P. L. Gai and P. Day // *Physica C* **152** (1988) 335.
[40] J. R. Clem // *Phys. Rev. B* **43** (1991) 7837.
[41] D. Dimos, P. Chandhari, J. Mannhart and F. K. LeGoues // *Phys. Rev. Lett.* **61** (1988) 219.
[42] D. Dimos, P. Chandhari and J. Mannhart // *Phys. Rev. B* **41** (1990) 4038.
[43] S. E. Babcock, X. Y. Cai, D. L. Kaiser and D. C. Larbalestier // *Nature* **347** (1990) 167.
[44] K. Salama, V. Selvamanickam and D.F. Lee, In: *Processing and Properties of High T_c Superconductors*, ed. by S. Jin (Singapore, World Scientific, Vol 1, 1992) p155.
[45] N. Tomita, M. Arai, E.Yanagisawa, T. Morimoto, H. Kitaguchi, H. Kumakura, K. Tagano and K. Nomura // *Cryogenics* **36** (1996) 485.
[46] D.U.Gubser, R.J. Soulen,T.Datta and D. Kirven // *IEEE Trans Appl. Superconduct.* **5** (1995) 1302.
[47] K. L. Zeisler-Mashl, T. L. Francavilla, and C. S. Pande // *Mater. Sci. Eng. B*, **B56** (1998) 53.
[48] A. Goyal, E. D. Specht, D. M. Kroeger, T. A. Mason, D. J. Dingley and G. N. Riley // *J. Electronic Materials* **24** (1995) 1865.
[49] Riley // *J. Electronic Materials* **24** (1995) 1865.
[50] G. N. Riley, A. P. Malozemoff, Q. Li, S. Fleshler and T. G. Holesinger // *JOM* **49** (1997) 24.
[51] C. S. Pande and R. A. Masumura // *Physica C* **314** (1997) 147.